Non-specific CD8$^+$ T cells and dendritic cells/macrophages participate in CD8$^+$ T cell-mediated cluster formation against malaria liver-stage infection

Running title: CD8$^+$ T and dendritic cells in liver-stage malaria

Masoud Akbari,[a]* Kazumi Kimura,[a] Ganchimeg Bayarsaikhan,[a] Daisuke Kimura,[a] Mana Miyakoda,[a] Smriti Juriasingani,[b] Masao Yuda,[c] Rogerio Amino,[d] Katsuyuki Yui [a]#

Division of Immunology, Department of Molecular Microbiology and Immunology, Graduate School of Biomedical Sciences, Nagasaki University, Nagasaki, Japan[a]; Department of Microbiology & Immunology, Western University, London, Ontario, Canada[b]; Department of Medical Zoology, Mie University, School of Medicine, Mie, Japan[c]; Unit of Malaria Infection & Immunity, Department of Parasites and Insect Vectors, Institut Pasteur, Paris, France[d]

[#] Address correspondence to Katsuyuki Yui, katsu@nagasaki-u.ac.jp.

*Present address: Masoud Akbari, Department of Microbiology & Immunology, London Health Science Center, University Hospital, Western University, London, ON, Canada.

Abstract

$CD8^+$ T cells are the major effector cells that protect against malaria liver-stage infection, forming clusters around *Plasmodium*-infected hepatocytes and eliminating parasites after prolonged interaction with these hepatocytes. We aimed to investigate roles of specific and non-specific $CD8^+$ T cells in cluster formation and protective immunity. To this end, we used *Plasmodium berghei* ANKA expressing ovalbumin, as well as $CD8^+$ T cells from transgenic mice expressing a T cell receptor specific for ovalbumin (OT-I) and $CD8^+$ T cells specific for an unrelated antigen, respectively. While antigen-specific $CD8^+$ T cells were essential for cluster formation, both antigen-specific and non-specific $CD8^+$ T cells joined the cluster. However, non-specific $CD8^+$ T cells did not significantly contribute to protective immunity. In the livers of infected mice, specific $CD8^+$ T cells expressed high levels of CD25, compatible with a local, activated effector phenotype. *In vivo* imaging of the liver revealed that specific $CD8^+$ T cells interact with $CD11c^+$ cells around infected hepatocytes. Depletion of $CD11c^+$ cells virtually eliminated the clusters in the liver, leading to a significant decrease in protection. These experiments reveal an essential role of hepatic $CD11c^+$ dendritic cells and presumably macrophages in the formation of $CD8^+$ T cell clusters around *Plasmodium*-infected hepatocytes. Once cluster formation is triggered by parasite-specific $CD8^+$ T cells, specific and unrelated activated $CD8^+$ T cells join the clusters in a chemokine and dendritic cell-dependent manner. Non-specific $CD8^+$ T cells seem to play a limited role in protective immunity against *Plasmodium* parasites.

Introduction

Malaria is a major infectious disease, with 212 million cases and 429,000 malaria-induced deaths in 2015 (1). In the life cycle of *Plasmodium* parasites, sporozoites are injected into the skin via infectious bites from mosquitoes and specifically arrest in the liver, where they invade hepatocytes (2). In the liver stage, parasites multiply and mature inside infected hepatocytes, generating thousands of merozoites that eventually lyse the hepatocytes and are released into circulation to initiate infection of the blood-stage and cause malaria (3). Liver infection takes approximately 2 days in rodent malaria models and 7–10 days in *Plasmodium falciparum*-infected humans, and it represents the bottleneck of parasite burden in mammalian infections, making it an attractive target for vaccine development. Immunization with radiation-attenuated sporozoites, genetically attenuated parasites, or sporozoite infection under a chloroquine shield can induce sterile immunity against sporozoite challenge (4). $CD8^+$ T cells are the major effector cells that mediate this protective immunity by recognizing *Plasmodium* antigens in association with MHC class I molecules on the infected hepatocytes (4-6). The effector mechanisms responsible for the elimination of intrahepatic parasites by antigen-specific $CD8^+$ T cells remain controversial, however, and studies have suggested that effector molecules of $CD8^+$ T cells, such as IFN-γ, TNF-α, TRAIL, perforin, and Fas ligand, are involved in a multifactorial, redundant manner, with their contributions also varying depending on the parasite and host species (7, 8). In addition, although dendritic cells, Kupffer cells, and liver sinusoidal endothelial cells (LSECs) have been shown to express MHC class I and class II as well as costimulatory molecules and are able to cross-present antigens to $CD8^+$ T cells (6, 9), the role of these cells in the activation of malaria-specific $CD8^+$ T cells in the liver is not clearly understood.

Studies using $CD8^+$ T cells that have defined specificity for *Plasmodium* antigens show that a very high number of antigen-specific $CD8^+$ T cells are required for sterile protection against liver-stage malaria (10). The percentage of antigen-specific memory $CD8^+$ T cells required for sterile protection is on the order of 1–2% of $CD8^+$ T cells in BALB/c mice and this requirement is even higher in C57BL/6 mice (11, 12). Intravital imaging of malaria-specific $CD8^+$ T cells has revealed that effector $CD8^+$ T cells are recruited to the liver after sporozoite infection by chemokine-mediated mechanisms, where they form clusters around infected hepatocytes and where parasites are eliminated following a prolonged interaction between infected hepatocytes and $CD8^+$ T cells (12, 13). Activated $CD8^+$ T cells of unrelated specificity are also recruited to the clusters (13). Upon an infectious mosquito bite, it is likely that, in addition to $CD8^+$ T cells that are specified for liver-stage malaria antigens, those that are specific to other antigens including mosquito antigens are also primed. In addition, other infectious diseases are also common in malaria endemic regions, and it is important to consider the influence of activated $CD8^+$ T cells that are not specific for *Plasmodium* antigens on the protective immunity against malaria parasites (10). However, it is not clear whether these non-specific $CD8^+$ T cells, which are recruited to the clusters around infected hepatocytes, participate in the elimination of parasites from the liver.

In this study, we used *Plasmodium berghei* ANKA expressing a model antigen, ovalbumin (OVA) epitope, as well as green fluorescent protein (GFP), hereafter referred to as PbA-gfpOVA, to evaluate the role of $CD8^+$ T cells with unrelated specificity in the

protective immune response against liver-stage malaria. Using this strategy, we found that protection was dependent on specific $CD8^+$ T cells, while those of unrelated specificity were barely involved in protection. In addition to $CD8^+$ T cells that were recruited to clusters around infected hepatocytes, dendritic cells were recruited to these clusters in the liver and played pivotal roles in cluster development around the infected hepatocytes.

Results

Clusters around infected hepatocytes include both antigen-specific and non-specific $CD8^+$ T cells

To examine the role of antigen-specific and non-specific $CD8^+$ T cells in the clearance of malaria liver infection, we utilized PbA-gfpOVA that expresses the model antigen OVA epitope, as well as OT-I $CD8^+$ T cells that recognize OVA, and 2C $CD8^+$ T cells that recognize an unrelated antigen, L^d (Fig. 1A). OT-I and 2C cells were activated *in vitro* and were adoptively transferred into C57BL/6 mice. Mice were then infected with PbA-gfpOVA sporozoites, and imaging of the liver was performed 44 h later using two-photon microscopy (14). Both OT-I and 2C cells joined clusters around hepatocytes infected with PbA-gfpOVA, as previously reported using a different parasite, mouse, and antigen (Fig. 1B, Supplemental Video 1) (12, 13). OT-I cells formed clusters when they were transferred alone or with 2C cells, while 2C cells were unable to form clusters alone, indicating that recognition of the OVA epitope by OT-I cells is required for the initiation of cluster formation (Fig. 1C). Once clusters were formed, similar numbers of OT-I and 2C cells were present in the clusters following a positive linear correlation (Fig. 1D). The

velocity of OT-I and 2C cells was similar, and those inside clusters were slower than those outside (Fig. 1E), suggesting that both OT-I and 2C cells were affected by the microenvironment inside the clusters. Overall, the data showed that OT-I and 2C cells were recruited to the clusters by similar mechanisms after the initiation of cluster formation mediated by OT-I cells.

Essential role of antigen-specific $CD8^+$ T cells in cluster formation and protection

To investigate whether recruitment of parasite-specific and non-specific $CD8^+$ T cells to the liver as well as to clusters after sporozoite infection is dependent on chemokine receptor signaling, OT-I and 2C cells were independently treated or untreated with pertussis toxin (PTX), an inhibitor of G-protein coupled signaling, and were transferred into C57BL/6 mice. In uninfected mice, numbers of OT-I and 2C cells in the liver declined after PTX treatment, while those of co-transferred but untreated cells were not affected (Fig. 2A). Next, mice were infected with PbA-gfpOVA sporozoites after T cell transfer, and numbers of OT-I and 2C cells in the liver and clusters were determined 44 h after infection. In the infected mice, both OT-I and 2C cell numbers increased nearly tenfold when compared with numbers in uninfected mice (Fig. 2B). When OT-I cells were treated with PTX, recruitment of both OT-I and 2C cells into the infected liver declined, while treatment of 2C cells did not affect recruitment of OT-I cells (Fig. 2B). The treatment of OT-I cells with PTX inhibited the formation of all T cell clusters, while that of 2C cells inhibited only their recruitment to the clusters of OT-I cells (Fig. 2C). These results demonstrate a basal-level accumulation of activated $CD8^+$ T cells in the livers of non-infected mice. This accumulation strongly increases after hepatic infection

in the presence of activated parasite-specific $CD8^+$ T cells, which triggers cluster formation of specific and non-specific cells. Both basal accumulation and accumulation in clusters after triggering by specific $CD8^+$ T cells are dependent on G-protein signaling, presumably via the recruitment and/or retention of cells through chemokine receptors.

We next asked whether 2C cells that were recruited to clusters had any role in protecting against malaria parasites in the liver. OT-I and/or 2C cells were transferred into C57BL/6 mice that were then infected with PbA-gfpOVA sporozoites, and the hepatic parasite burden was determined. Transfer of OT-I cells reduced the parasite burden in the liver, while that of 2C cells alone did not have any significant effect (Fig. 3A). We next mixed different doses of 2C cells with OT-I cells and co-transferred them into mice infected with PbA-gfpOVA sporozoites. The addition of 2C cells did not significantly contribute to the reduction in parasite burden by OT-I cells when they were transferred into mice at the same dose (2.5×10^6) (Fig. 3B) or at a dose 5 times higher (15.0×10^6) (Fig. 3A). We concluded that under our experimental conditions, protective immunity against liver-stage infection depends on *Plasmodium*-specific $CD8^+$ T cells and that non-specific activated $CD8^+$ T cells did not significantly contribute to protection, although they did join the cellular clusters initiated by specific $CD8^+$ T cells around infected hepatocytes.

Activation status of specific $CD8^+$ T cells in the infected liver

Since both specific and non-specific cells were recruited to the OT-I-dependent clusters around infected hepatocytes, we examined the numbers of these cells in the livers of infected mice. The numbers of OT-I and 2C cells increased dramatically in the livers

157 but not the spleens of mice infected with PbA-gfpOVA (Fig. 4B, C). The number of
158 host $CD8^+$ T cells was not elevated in the liver, suggesting that activated OT-I and 2C
159 cells were attracted to the microenvironment of the infected liver. To examine the
160 activation status of OT-I and 2C cells that were recruited into the liver, we examined the
161 expression of CD25 and CD69 on $CD8^+$ T cells (Fig. 4). Interestingly, the expression
162 of CD25 on OT-I cells was significantly higher than that on 2C cells in the infected liver,
163 although CD69 expression was similar (data not shown). This high CD25 expression
164 was not seen in OT-I cells in the spleen, suggesting that OT-I cells in the infected liver
165 were activated.

166

167 Since OT-I cells in the liver express CD25 at higher levels than 2C cells in infected mice,
168 we hypothesized that they were activated via the recognition of OVA epitope in the
169 hepatic environment. To visualize interactions among dendritic cells, specific $CD8^+$ T
170 cells, and infected cells in the liver, OT-I cells were transferred into CD11c-eYFP mice,
171 which were subsequently infected with PbA-gfpOVA sporozoites. In the hepatic myeloid
172 cells, $CD11c^+$ cells consisted of $CD11c^+F4/80^-$ dendritic cells and $CD11c^+F4/80^+$ cells
173 that are likely to be a subpopulation of Kupffer cells (15). Intravital imaging showed that
174 $CD11c^+$ cells were present in clusters around infected hepatocytes and that OT-I cells
175 around the infected hepatocytes were in close contact with them (Fig. 5A, B,
176 Supplemental Video 2, 3). This pervasive presence of $CD11c^+$ cells in clusters and their
177 close association with $CD8^+$ T cells suggest that they might play a role in cluster
178 formation. To examine the role of $CD11c^+$ cells in the formation of clusters of OT-I cells,
179 OT-I cells were transferred into CD11c-DTR chimeric mice that were then infected with

PbA-gfpOVA sporozoites. In the liver of chimeric mice into which OT-I cells were transferred and infected with PbA-OVA, the number of $CD11c^+$MHC II^+ dendritic cells increased when compared with those that did not receive OT-I cells (Fig. 5C). Treatment of these mice with diphtheria toxin (DTX) resulted in a dramatic reduction in the number of $CD11c^+$ cells in both the liver and spleen (Fig. 5C). After the depletion of $CD11c^+$ cells, the numbers of $CD8^+$ T cells and OT-I cells in the liver were severely diminished, while those in the spleen were not affected (Fig. 5D). Imaging of the liver showed that the number of OT-I clusters were severely reduced after the depletion of $CD11c^+$ cells (Fig. 5E). This reduction in the number of clusters was not due to the direct toxic effect of DTX on the parasites, since the parasite burden in the livers of mice without OT-I cells was not affected by DTX treatment (Fig. 5F). Furthermore, the expression of CD25 on OT-I cells in the liver after infection was diminished in mice depleted of $CD11c^+$ cells (Fig. 5G), suggesting that the CD25 expression on OT-I cells in the liver in PbA-gfpOVA-infected mice was, at least in part, dependent on $CD11c^+$ cells in the liver. Therefore, we examined whether the protective effect of OT-I cells against PbA-gfpOVA sporozoite infection was altered by DTX treatment (Fig. 5H). Depletion of $CD11c^+$ cells resulted in reduced protection elicited by OT-I cells, which correlated with the numbers of OT-I cells in the liver.

Discussion

$CD8^+$ T cells are major effector cells in the protective immune response against malaria liver-stage infection. Both parasite-specific and non-specific activated $CD8^+$ T cells form clusters around infected hepatocytes during the protective immune response (12, 13). We

used OVA as a model antigen, as well as OT-I and 2C T cell receptor (TCR) transgenic T cells as antigen-specific and non-specific $CD8^+$ T cells, respectively, to study the mechanisms underlying the formation of clusters of $CD8^+$ T cells and their role in the protective immune response against OVA-expressing malaria in the liver stage. We activated OT-I and 2C cells *in vitro* prior to their transfer into mice, since naïve $CD8^+$ T cells did not accumulate in the liver and were not protective against PbA-gfpOVA infection (data not shown) (16). The initiation of cluster formation was tightly regulated by the recognition of antigens by specific $CD8^+$ T cells, suggesting that the recruitment of activated $CD8^+$ T cells to infected hepatocytes is initiated by the recognition of parasite antigens by activated malaria antigen-specific $CD8^+$ T cells. However, activated non-specific $CD8^+$ T cells joined these clusters in a manner independent of TCR recognition. The expression of chemokine receptors or adhesion molecules on activated $CD8^+$ T cells may be sufficient for their recruitment into clusters of $CD8^+$ T cells, as shown previously (13, 17), although the chemokine that is required for the migration of $CD8^+$ T cells to the liver during malaria infection has not been identified. However, under our experimental conditions, the non-specific $CD8^+$ T cells in these clusters did not significantly contribute to protection, indicating that TCR-mediated signaling is required for directing the effector function of $CD8^+$ T cells towards infected hepatocytes. In malaria endemic regions, the population is constantly exposed to various infectious microbes, and may possess circulating effector T cells non-specific to malaria antigens. In addition, mosquito antigen-specific $CD8^+$ T cells may also be induced upon an infectious bite. Our study suggests that these non-specific T cells may join the cluster, but will not directly contribute to protective immunity at the liver stage of *Plasmodium* infection. TCR sharing of bystander $CD8^+$ T cells does not appear to take place in liver-stage infection (18). It

will be intriguing to determine whether the recruitment of non-specific activated T cells with different profiles of anti-liver-stage cytokine secretion (19-21) to the cluster enhances the elimination of infected cells.

$CD11c^+$ cells in hepatic myeloid cells consist of at least two subpopulations, $CD11c^+F4/80^-$ and $CD11c^+F4/80^+$ cells, which are mostly dendritic cells and a subpopulation of Kupffer cells, respectively (15). We found that $CD11c^+$ cells increased in mice into which OT-I cells were transferred and infected with PbA-OVA, and accumulated in the clusters of activated $CD8^+$ T cells that were formed around the infected hepatocytes. The recruitment of $CD11c^+$ cells may be triggered by the infected hepatocytes, which recognize *Plasmodium* parasites via receptors for pathogen-associated molecular patterns in a type I interferon (IFN)-dependent, and thus activated $CD8^+$ T cell-independent, manner (22, 23). However, since cluster formation is dependent on specific $CD8^+$ T cells, it is more likely that OT-I cells recruit $CD11c^+$ cells following the recognition of infected hepatocytes. When $CD11c^+$ cells were depleted by DTX treatment in CD11c-DTR chimeric mice, the formation of $CD8^+$ T cell clusters was strongly reduced, implying that $CD11c^+$ cells in the liver play a pivotal role in the orchestration of cluster formation. The depletion of $CD11c^+$ cells significantly decreased the protection conferred by the transfer of OT-I cells, correlating with the decrease in OT-I cell numbers in the liver suggesting that $CD11c^+$ dendritic cells in the cluster have pivotal roles for the effector function of these specific $CD8^+$ T cells in protection. Alternatively, there is a possibility for a direct protective role of $CD11c^+$ cells in the clusters via cytokine secretion or phagocytosis, because targeting of $CD11c^+$ cells with DTX depletes a majority of $CD11c^+$ dendritic cells and a significant proportion

of $CD11c^+F4/80^+$ Kupffer cells (15). However, $CD11c^-F4/80^+$ Kupffer cells should remain intact in DTX-treated mice, and we believe that this possibility is less likely.

In our imaging study, we observed that OT-I cells that approached clusters around infected hepatocytes were closely associated with $CD11c^+$ cells. These results suggest that $CD11c^+$ cells that were recruited to infected hepatocytes form a microenvironment that attracts activated $CD8^+$ T cells, increasing the opportunity for antigen-specific $CD8^+$ T cells to recognize and eliminate the infected hepatocytes. $CD11c^+$ dendritic cells are known to cross-present antigens to specific $CD8^+$ T cells when in close contact. In the liver of mice infected with radiation-attenuated *Plasmodium* sporozoites, $CD8\alpha^+$ dendritic cells present liver-stage antigens to activate effector $CD8^+$ T cells (24). However, it was reported that effector $CD8^+$ cells do not require bone marrow-derived antigen presenting cells for protection at the liver-stage of *P. yoelii* infection (25). Furthermore, dendritic cells use the endosome-cytosol pathway to cross-present *Plasmodium* antigens to $CD8^+$ T cells, and this endosomal pathway of antigen presentation has been shown to be dispensable for the protective immunity against infected hepatocytes mediated by activated specific $CD8^+$ T cells (26). Thus, we believe that this pathway is unlikely to be essential for protection in the liver, although it may have an ancillary role. An alternative possibility is that specific $CD8^+$ T cells directly receive activation signals upon recognition of the antigens presented on infected hepatocytes via their TCR. Under this scenario, $CD11c^+$ cells that are recruited to infected hepatocytes do not directly activate specific $CD8^+$ T cells but may attract activated $CD8^+$ T cells to the infected hepatocytes in an antigen-non-specific manner via the expression of adhesion molecules and secretion of chemokines.

We observed clusters of $CD8^+$ T cells 44 h after infection with sporozoites, representing a relatively late period of liver-stage infection. At this late time, $CD8^+$ T cell clusters were heterogeneous, including the accumulation of a few $CD8^+$ T cells around infected hepatocytes to large clusters of hundreds of $CD8^+$ T cells that accumulated after the elimination of parasites. Our study demonstrated the critical role of dendritic cells in the formation of these $CD8^+$ T cells clusters and their impact on protection. In addition, we showed that *Plasmodium*-specific $CD8^+$ T cells within the cluster are likely involved in the elimination of infected cells. It is well known that the activation of innate immunity is critical for the induction of adaptive immune responses (27). Our study highlights the important role of innate immune cells in inducing the effector mechanisms of activated $CD8^+$ T cells during the liver stage of *Plasmodium* infection. Further study will reveal the molecular mechanisms underlying the interaction between dendritic cells and effector $CD8^+$ T cells that play essential roles in the elimination of liver-stage *Plasmodium*.

Materials and Methods

Animals

OT-I transgenic mice expressing a TCR specific for $OVA_{257-264}/K^b$ were obtained from Dr. H. Kosaka (Osaka University, Osaka, Japan) (28). B6.SJL and OT-I mice were interbred, and the offspring were intercrossed to obtain $CD45.1^+$ OT-I mice. In addition, 2C mice (29) (RBRC00123) were provided by RIKEN BRC through the National Bio-Resource Project of the Ministry of Education, Culture, Sports, Science and Technology,

Japan. DsRed.T3 (30), CD11c-DTR (31), and CD11c-eYFP (32) transgenic mice were purchased from The Jackson Laboratory (Bar Harbor, ME). B6-EGFP (GFP) and C57BL/6 mice were purchased from SLC (Shizuoka, Japan). OT-I mice were interbred with DsRed.T3 and GFP transgenic mice to generate DsRed/OT-I and GFP/OT-I mice, respectively, while 2C mice were crossed with DsRed.T3 mice to generate DsRed/2C mice. Mice were maintained in the Laboratory Animal Core for Animal Research at Nagasaki University and were used at the age of 8–14 weeks. The animal experiments represented here were approved by the Institutional Animal Care and Use Committee of Nagasaki University and were conducted according to the Guidelines for Animal Experimentation at Nagasaki University.

T-cell transfer, parasite infection, and imaging

For the preparation of activated OT-I cells, cells were harvested from the spleens and inguinal lymph nodes of OT-I mice and were pulsed with $OVA_{257-264}$ peptide (2 μg/ml) for 4 h, washed, and cultured for 3 days. For 2C cells, cells were prepared from DsRed/2C mice and were pulsed with 2C SIYRYYGL peptide (5 μg/ml) (33). Mice received activated OT-I or 2C cells ($5–10 \times 10^6$) intravenously through the tail vein.

Activated OT-I and 2C $CD8^+$ T cells were treated with PTX (100 ng/ml; Sigma, St. Louis, MO) for 3 h at 37 °C and washed three times with phosphate-buffered saline (PBS) before transfer to mice. Each type of cell (OT-I and 2C, PTX-treated and untreated) was transferred separately into the recipient mouse.

PbA-gfpOVA sporozoites were collected from the salivary glands of infected *Anopheles stephensi* mosquitoes. One day after cell transfer, mice were intravenously infected with PbA-gfpOVA sporozoites (1×10^4). Then, 44 h after infection, the liver was imaged using an inverted TCS SP5 two-photon microscope equipped with an OPO laser (Leica, Microsystem, Wetzlar, Germany) with a 25× water immersion objective as described (12, 14). Analysis of two-photon imaging data was performed using Imaris 7.6.5 software (Bitplane, Zurich, Switzerland).

Liver cell suspension

The liver cell suspension was prepared as described previously with modifications (34). Briefly, the isolated liver was crushed by a syringe plunger in a petri dish placed on ice in 5 ml PBS. The cell suspension was centrifuged, and the pellet was suspended in a solution of 33% Percoll in PBS and centrifuged at 800 × *g* for 30 min at 20 °C. Parenchymal cells and debris on the top were removed using a glass pipet, and the pellet was suspended in Gey's solution to lyse red blood cells, centrifuged, washed with PBS, re-suspended in PBS, and stained with fluorochrome-conjugated antibodies.

Flow cytometry

Cells were blocked with anti-CD16/CD32 (2.4G2) and incubated with antibodies specific for CD8α and CD25 (eBioscience, San Diego, CA) as described previously (12). All samples were analyzed using BD FACSCanto II or BD LSRFortessa X-20 (BD Biosciences, San Jose, CA). Data were analyzed using FlowJo software v10.2

(TreeStar, Ashland, OR). The difference in mean fluorescent intensity (ΔMFI) was used to determine the difference between experimental staining and isotype control.

Real-time PCR to determine parasite burden

Total liver RNA was isolated using Isogen II (Nippon Gene, Tokyo, Japan) 44 h after infection with 10,000 PbA-gfpOVA sporozoites. RNA was treated with DNase (Takara, Kusatsu, Japan) according to the manufacturer's protocol and was separated on 1% agarose gel to verify its integrity using the ratio of 28S to 18S rRNA. Complementary DNA was prepared from 2 μg of RNA and amplified by PCR using primer pairs targeted to the 18S rRNA sequence of *Plasmodium yoelii* (35) or mouse (36) in a mixture containing SYBR Green (Applied Biosystems, Foster City, CA). Samples were amplified by an ABI PRISM 7900HT automatic real-time RT-PCR system (Applied Biosystems). The threshold cycle of each PCR was converted into a DNA equivalent using standard curves made by amplifying tenfold dilutions of a plasmid bearing the relevant target sequences. Liver parasite burden was determined as the ratio of cDNA equivalent measured for *P. yoelii* 18S rRNA to that for mouse 18S.

Depletion of $CD11c^+$ cells

C57BL/6 mice were lethally irradiated (900 rad) and intravenously received bone marrow cells from CD11c-DTR mice (1.0×10^7) on the following day to generate bone marrow chimeric (CD11c-DTR chimeric) mice. Mice were maintained for more than two months before infection to allow reconstitution of the hematopoietic cells. To deplete

dendritic cells, CD11c-DTR chimeric mice were intraperitoneally injected with 0.5 μg/mouse DTX in 1 ml PBS 2 h after infection with sporozoites.

Statistical analysis

In comparisons between two groups, unpaired two-tailed Student's *t*-tests were used. In comparison of three or more groups, an overall difference was first made by a one-way or two-way ANOVA followed by Sidak's multiple comparison tests. Statistical analysis was performed using GraphPad Prism version 6 (GraphPad Software, San Diego, CA, USA). Correlations were analyzed using Spearman's rank correlation coefficient. * $p \leq 0.05$. Results are presented as mean ± SD.

Acknowledgments

We thank Ms. Kawamoto and Ms. Yoshida for their technical assistance. This work was supported by grants-in-aid for scientific research from the Japan Society for the Promotion of Science (25113717,15K15124) to KY.

Disclosures

The authors have no financial conflicts of interest.

References

1. **WHO.** 2017. World malaria report 2016.
2. **Tavares J, Costa DM, Teixeira AR, Cordeiro-da-Silva A, Amino R.** 2017. In vivo imaging of pathogen homing to the host tissues. Methods **127:**37-44.
3. **Menard R, Tavares J, Cockburn I, Markus M, Zavala F, Amino R.** 2013. Looking under the skin: the first steps in malarial infection and immunity. Nat Rev Microbiol **11:**701-712.
4. **Hafalla JC, Silvie O, Matuschewski K.** 2011. Cell biology and immunology of malaria. Immunol Rev **240:**297-316.
5. **Schofield L, Villaquiran J, Ferreira A, Schellekens H, Nussenzweig R, Nussenzweig V.** 1987. γInterferon, $CD8^+$ T cells and antibodies required for immunity to malaria sporozoites. Nature **330:**664-666.
6. **Frevert U, Nacer A.** 2013. Immunobiology of *Plasmodium* in liver and brain. Parasite Immunol **35:**267-282.
7. **Morrot A, Zavala F.** 2004. Effector and memory $CD8^+$ T cells as seen in immunity to malaria. Immunol Rev **201:**291-303.
8. **Butler NS, Schmidt NW, Harty JT.** 2010. Differential effector pathways regulate memory CD8 T cell immunity against *Plasmodium berghei* versus *P. yoelii* sporozoites. J Immunol **184:**2528-2538.
9. **Thomson AW, Knolle PA.** 2010. Antigen-presenting cell function in the tolerogenic liver environment. Nat Rev Immunol **10:**753-766.
10. **Schmidt NW, Harty JT.** 2011. Cutting edge: attrition of *Plasmodium*-specific memory CD8 T cells results in decreased protection that is rescued by booster immunization. J Immunol **186:**3836-3840.
11. **Van Braeckel-Budimir N, Harty JT.** 2014. CD8 T-cell-mediated protection against liver-stage malaria: lessons from a mouse model. Front Microbiol **5:**272.

12. **Kimura K, Kimura D, Matsushima Y, Miyakoda M, Honma K, Yuda M, Yui K.** 2013. $CD8^+$ T cells specific for a malaria cytoplasmic antigen form clusters around infected hepatocytes and are protective at the liver stage of infection. Infect Immun **81:**3825-3834.

13. **Cockburn IA, Amino R, Kelemen RK, Kuo SC, Tse SW, Radtke A, Mac-Daniel L, Ganusov VV, Zavala F, Menard R.** 2013. In vivo imaging of $CD8^+$ T cell-mediated elimination of malaria liver stages. Proc Natl Acad Sci U S A **110:**9090-9095.

14. **Akbari M, Kimura K, Houts JT, Yui K.** 2016. Intravital imaging of the immune responses during liver-stage malaria infection: An improved approach for fixing the liver. Parasitol Int **65:**502-505.

15. **David BA, Rezende RM, Antunes MM, Santos MM, Freitas Lopes MA, Diniz AB, Sousa Pereira RV, Marchesi SC, Alvarenga DM, Nakagaki BN, Araujo AM, Dos Reis DS, Rocha RM, Marques PE, Lee WY, Deniset J, Liew PX, Rubino S, Cox L, Pinho V, Cunha TM, Fernandes GR, Oliveira AG, Teixeira MM, Kubes P, Menezes GB.** 2016. Combination of mass cytometry and imaging analysis reveals origin, location, and functional repopulation of liver myeloid cells in mice. Gastroenterology **151:**1176-1191.

16. **John B, Crispe IN.** 2004. Passive and active mechanisms trap activated $CD8^+$ T cells in the liver. J Immunol **172:**5222-5229.

17. **Tse SW, Radtke AJ, Espinosa DA, Cockburn IA, Zavala F.** 2014. The chemokine receptor CXCR6 is required for the maintenance of liver memory $CD8^+$ T cells specific for infectious pathogens. J Infect Dis **210:**1508-1516.

18. **Chaudhri G, Quah BJ, Wang Y, Tan AH, Zhou J, Karupiah G, Parish CR.** 2009. T cell receptor sharing by cytotoxic T lymphocytes facilitates efficient virus control. Proc Natl Acad Sci U S A **106:**14984-14989.

19. **Ferreira A, Schofield L, Enea V, Schellekens H, van der Meide P, Collins WE, Nussenzweig RS, Nussenzweig V.** 1986. Inhibition of development of exoerythrocytic forms of malaria parasites by γ-interferon. Science **232:**881-884.

20. **Nussler A, Pied S, Goma J, Renia L, Miltgen F, Grau GE, Mazier D.** 1991. TNF inhibits malaria hepatic stages in vitro via synthesis of IL-6. Int Immunol **3:**317-321.

21. **Schmieg J, Yang G, Franck RW, Tsuji M.** 2003. Superior protection against malaria and melanoma metastases by a C-glycoside analogue of the natural killer T cell ligand α-Galactosylceramide. J Exp Med **198:**1631-1641.

22. **Liehl P, Zuzarte-Luis V, Chan J, Zillinger T, Baptista F, Carapau D, Konert M, Hanson KK, Carret C, Lassnig C, Muller M, Kalinke U, Saeed M, Chora AF, Golenbock DT, Strobl B, Prudencio M, Coelho LP, Kappe SH, Superti-Furga G, Pichlmair A, Vigario AM, Rice CM, Fitzgerald KA, Barchet W, Mota MM.** 2014. Host-cell sensors for *Plasmodium* activate innate immunity against liver-stage infection. Nat Med **20:**47-53.

23. **Miller JL, Sack BK, Baldwin M, Vaughan AM, Kappe SH.** 2014. Interferon-mediated innate immune responses against malaria parasite liver stages. Cell Rep **7:**436-447.

24. **Jobe O, Donofrio G, Sun G, Liepinsh D, Schwenk R, Krzych U.** 2009. Immunization with radiation-attenuated *Plasmodium berghei* sporozoites induces liver cCD8α^+ DC that activate CD8$^+$ T cells against liver-stage malaria. PLoS One **4:**e5075.

25. **Chakravarty S, Cockburn IA, Kuk S, Overstreet MG, Sacci JB, Zavala F.** 2007. CD8$^+$ T lymphocytes protective against malaria liver stages are primed in skin-draining lymph nodes. Nat Med **13:**1035-1041.

26. **Cockburn IA, Tse SW, Radtke AJ, Srinivasan P, Chen YC, Sinnis P, Zavala F.** 2011. Dendritic cells and hepatocytes use distinct pathways to process protective antigen from *Plasmodium* in vivo. PLoS Pathog **7:**e1001318.

460 27. **Iwasaki A, Medzhitov R.** 2015. Control of adaptive immunity by the innate immune
461 system. Nat Immunol **16:**343-353.
462 28. **Hogquist KA, Jameson SC, Heath WR, Howard JL, Bevan MJ, Carbone FR.** 1994.
463 T cell receptor antagonist peptides induce positive selection. Cell **76:**17-27.
464 29. **Sha WC, Nelson CA, Newberry RD, Kranz DM, Russell JH, Loh DY.** 1988. Selective
465 expression of an antigen receptor on CD8-bearing T lymphocytes in transgenic mice.
466 Nature **335:**271-274.
467 30. **Vintersten K, Monetti C, Gertsenstein M, Zhang P, Laszlo L, Biechele S, Nagy A.**
468 2004. Mouse in red: red fluorescent protein expression in mouse ES cells, embryos, and
469 adult animals. Genesis **40:**241-246.
470 31. **Jung S, Unutmaz D, Wong P, Sano G, De los Santos K, Sparwasser T, Wu S,**
471 **Vuthoori S, Ko K, Zavala F, Pamer EG, Littman DR, Lang RA.** 2002. In vivo
472 depletion of $CD11c^+$ dendritic cells abrogates priming of $CD8^+$ T cells by exogenous cell-
473 associated antigens. Immunity **17:**211-220.
474 32. **Lindquist RL, Shakhar G, Dudziak D, Wardemann H, Eisenreich T, Dustin ML,**
475 **Nussenzweig MC.** 2004. Visualizing dendritic cell networks in vivo. Nat Immunol
476 **5:**1243-1250.
477 33. **Udaka K, Tsomides TJ, Eisen HN.** 1992. A naturally occurring peptide recognized by
478 alloreactive $CD8^+$ cytotoxic T lymphocytes in association with a class I MHC protein.
479 Cell **69:**989-998.
480 34. **Watarai H, Nakagawa R, Omori-Miyake M, Dashtsoodol N, Taniguchi M.** 2008.
481 Methods for detection, isolation and culture of mouse and human invariant NKT cells.
482 Nat Protoc **3:**70-78.
483 35. **Kawabata Y, Udono H, Honma K, Ueda M, Mukae H, Kadota J, Kohno S, Yui K.**
484 2002. Merozoite surface protein 1-specific immune response is protective against
485 exoerythrocytic forms of *Plasmodium yoelii*. Infect Immun **70:**6075-6082.

36. **Kimura D, Miyakoda M, Kimura K, Honma K, Hara H, Yoshida H, Yui K.** 2016. Interleukin-27-producing $CD4^+$ T cells regulate protective immunity during malaria parasite infection. Immunity **44:**672-682.

Figure legends

Figure 1. Both antigen-specific and non-specific $CD8^+$ T cells join clusters around infected hepatocytes. (A) Experimental design of two-photon imaging of antigen-specific (GFP/OT-I) and non-specific (DsRed/2C) $CD8^+$ T cells in the liver after sporozoite infection. (B)Time-lapse two-photon images of OT-I cells (green) and 2C cells (red) in a cluster formed in the liver. The yellow dashed circle shows the arbitrary border of a cluster. Arrowheads indicate OT-I and 2C cells outside the cluster moving towards the cluster. (C) Number of clusters in 132-mm^2 image fields from the livers of mice treated with OT-I, 2C, or both OT-I and 2C cells (n = 3 mice/group). Each dot represents one mouse. *$p < 0.05$; ns, not significant by one-way ANOVA followed by Sidak's multiple comparison tests. (D) Number of OT-I and 2C cells located inside each cluster. Each dot represents one cluster. $p < 0.0001$ by Spearman's rank correlation coefficient. (E) The velocity of OT-I and 2C cells inside and outside of clusters. Each dot represents one $CD8^+$ T cell. Data are derived from five experiments with similar results. *$p < 0.05$; ns, not significant by two-way ANOVA followed by Sidak's multiple comparison tests.

Figure 2. Antigen-specific $CD8^+$ T cells initiate the recruitment of activated $CD8^+$ T cells. Activated OT-I and 2C cells were incubated with (+) or without (-) PTX and transferred to B6 mice. The mice were uninfected (A) or infected (B) with PbA-

gfpOVA sporozoites, and cell numbers in the liver were determined by flow cytometry. Each dot represents one mouse. (C) After infection with PbA-gfpOVA, numbers of OT-I and 2C cells in individual clusters were determined using two-photon microscopy. Each dot represents one cluster. The values of OT-I and 2C cells in the same mouse (A, B) or in the same cluster (C) are connected by a line. Data are representative of three experiments with similar results. *$p < 0.05$; ns, not significant by two-way ANOVA followed by Sidak's multiple comparison tests.

Figure 3. Antigen non-specific $CD8^+$ T cells contribute little to protective immunity. C57BL/6 mice were treated with or without activated OT-I ($2.5–15.0 \times 10^6$) or 2C ($2.5–15.0 \times 10^6$) cells and were infected (+) or not infected (-) with PbA-gfpOVA sporozoites; after 44 h, the parasite burden in the liver was determined by real-time PCR. Numbers of transferred OT-I and 2C cells are indicated. Each dot represents one mouse. A and B show two representative experiments from a total of nine replicates. *$p < 0.05$; ns, not significant by one-way ANOVA followed by Sidak's multiple comparisons.

Figure 4. Accumulation and activation of $CD8^+$ T cells in the livers of infected mice. C57BL/6 mice were treated with activated GFP/OT-I and DsRed/2C cells and infected or not infected with PbA-gfpOVA; then, single-cell suspensions from the liver were stained for CD8 and CD25 at 44 h after infection. (A) After gating for $CD8^+$ cells and for GFP vs. DsRed, CD25 (orange) and isotype control (gray) profiles of OT-I ($CD8^+GFP^+$), 2C ($CD8^+DsRed^+$), and host $CD8^+$ ($CD8^+GFP^-DsRed^-$) cells are shown. Numbers in the flow cytometry profiles indicate the proportion (%) of the population. Numbers and CD25

532 expression of OT-I, 2C, and host $CD8^+$ T cells in the livers (B) and spleens (C) of
533 uninfected and infected mice are plotted. The expression levels of CD25 are shown as
534 the differences in mean fluorescence intensity of anti-CD25 antibody staining and isotype
535 controls (ΔMFI). Each dot represents one mouse. Data are representative of two
536 experiments with similar results. * $p < 0.05$; ns, not significant by two-way ANOVA
537 followed by Sidak's multiple comparison tests.

538

539 **Figure 5.** Dendritic cells play a pivotal role in the formation of $CD8^+$ T cell clusters.
540 (A, B) CD11c-eYFP mice were transferred with activated DsRed/OT-I cells and infected
541 with PbA-gfpOVA sporozoites, and liver imaging was performed using two-photon
542 microscopy. (A) Time-lapse images of OT-I cells (red cells, small yellow arrowheads)
543 associated with $CD11c^+$ cells (green) around infected hepatocytes (yellow, large white
544 arrowhead). (B) Image CD11c-eYFP cells (green) in a cluster (left) and overlay image
545 of OT-I (red) and $CD11c^+$ cells (green) in the same cluster (right).

546 (C–H) CD11c-DTR chimeric mice were transferred (+) or not transferred (-) with
547 activated OT-I cells, infected with PbA-gfpOVA sporozoites except one group in (G),
548 and treated (+) or not treated (-) with DTX. (C) Liver and spleen cells were stained, and
549 analyzed using flow cytometry. The proportions (%) of $MHCII^+CD11c^+$ dendritic cells
550 are shown from $CD45.2^+$ liver (Upper) and spleens (Lower) cells (Left), and their
551 absolute numbers were calculated (Right). (D) Total numbers of suspended cells (left)
552 and OT-I cells (right) in the liver (upper) and spleen (lower) were determined. (E) Livers
553 were examined under two-photon microscope 44 h after infection, and the numbers of
554 clusters in a 132-mm^2 area were determined. (F) Parasite burden in mice treated with

555 higher (0.1 μg) and lower (0.05 μg) doses of DTX without OT-I transfer was determined
556 by real time-PCR. The proportion (%) of $CD25^+$ cells in OT-I cells in liver cell
557 suspension (G) and parasite burden in the liver (H) were determined 44 h after infection
558 (+) or without infection (-). Each dot represents one mouse. Data are representative
559 of three experiments with similar results. Results are presented as mean ± SD. *$p <$
560 0.05; ns, not significant by unpaired *t*-tests (D right, E). *$p < 0.05$; ns, not significant by
561 one-way-ANOVA (C, D left, F-H) followed by Sidak's multiple comparison tests.

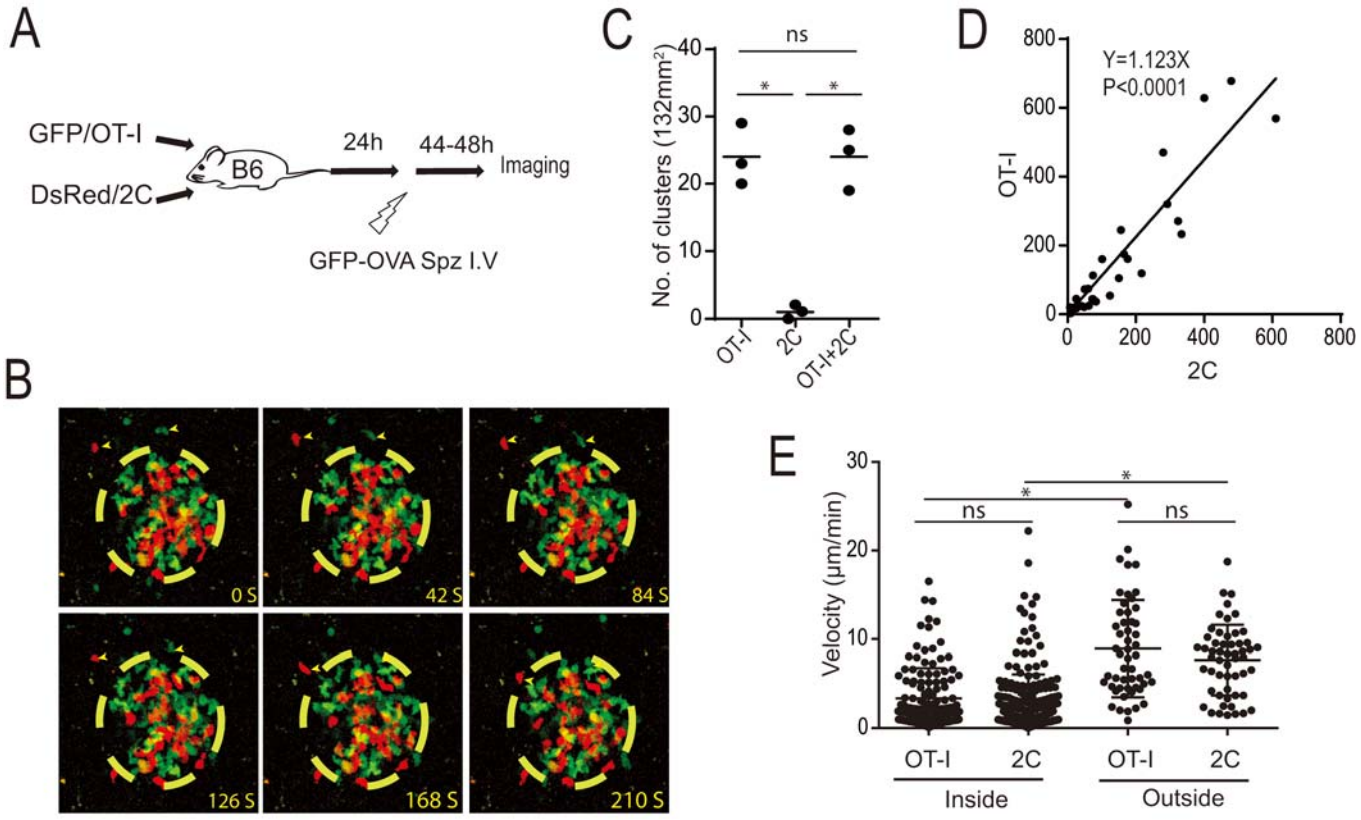
A
GFP/OT-I
DsRed/2C
B6
24h
44-48h
Imaging
GFP-OVA Spz I.V
B
0 S
42 S
84 S
126 S
168 S
210 S
C
No. of clusters (132mm²)
ns
*
*
OT-I
2C
OT-I+2C
D
Y=1.123X
P<0.0001
OT-I
2C
E
Velocity (µm/min)
ns
*
*
ns
OT-I
2C
OT-I
2C
Inside
Outside

Fig. 1

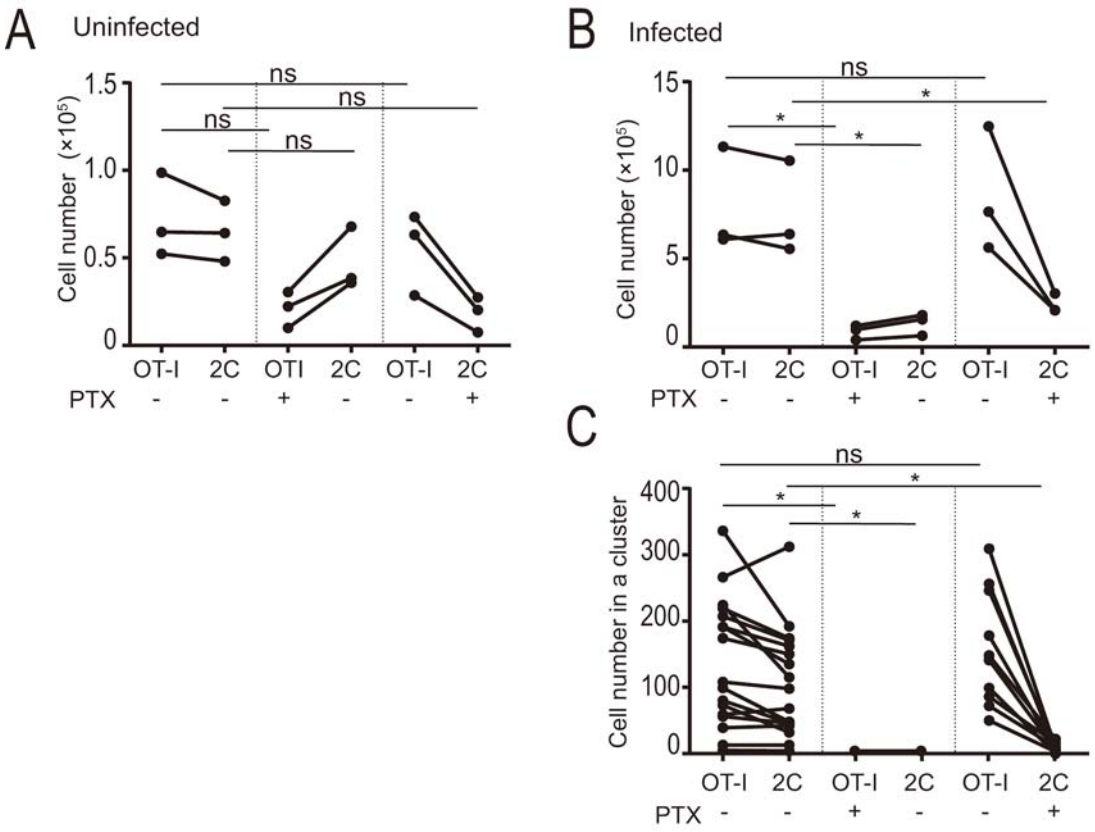
A
Uninfected
Cell number (×10^5)
1.5
1.0
0.5
0
ns
ns
ns
ns
OT-I 2C OTI 2C OT-I 2C
PTX - - + - - +
B
Infected
Cell number (×10^5)
15
10
5
0
ns
*
*
*
OT-I 2C OT-I 2C OT-I 2C
PTX - - + - - +
C
Cell number in a cluster
400
300
200
100
0
ns
*
*
*
OT-I 2C OT-I 2C OT-I 2C
PTX - - + - - +

Fig. 2

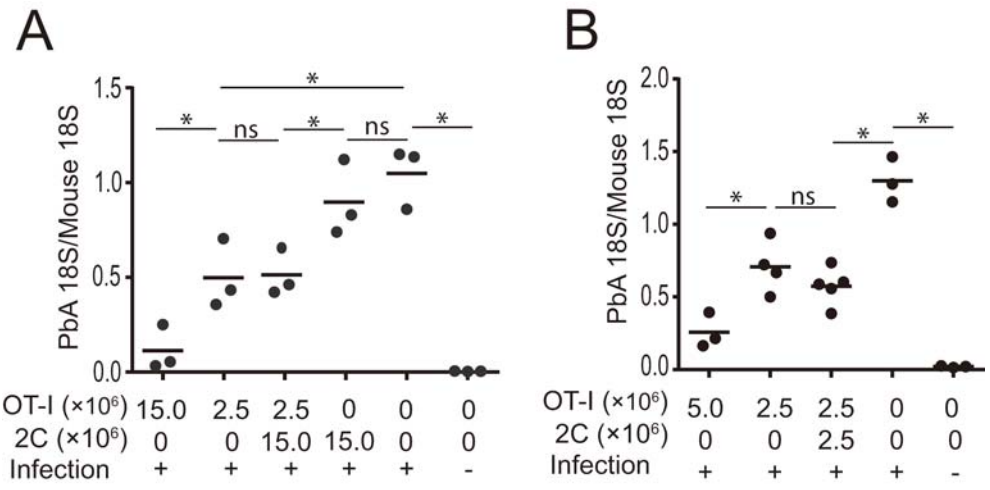
A
PbA 18S/Mouse 18S
1.5
1.0
0.5
0.0
*
ns
*
ns
*
*
OT-I (×10⁶) 15.0 2.5 2.5 0 0 0
2C (×10⁶) 0 0 15.0 15.0 0 0
Infection + + + + + -
B
PbA 18S/Mouse 18S
2.0
1.5
1.0
0.5
0.0
*
ns
*
*
OT-I (×10⁶) 5.0 2.5 2.5 0 0
2C (×10⁶) 0 0 2.5 0 0
Infection + + + + -

Fig. 3

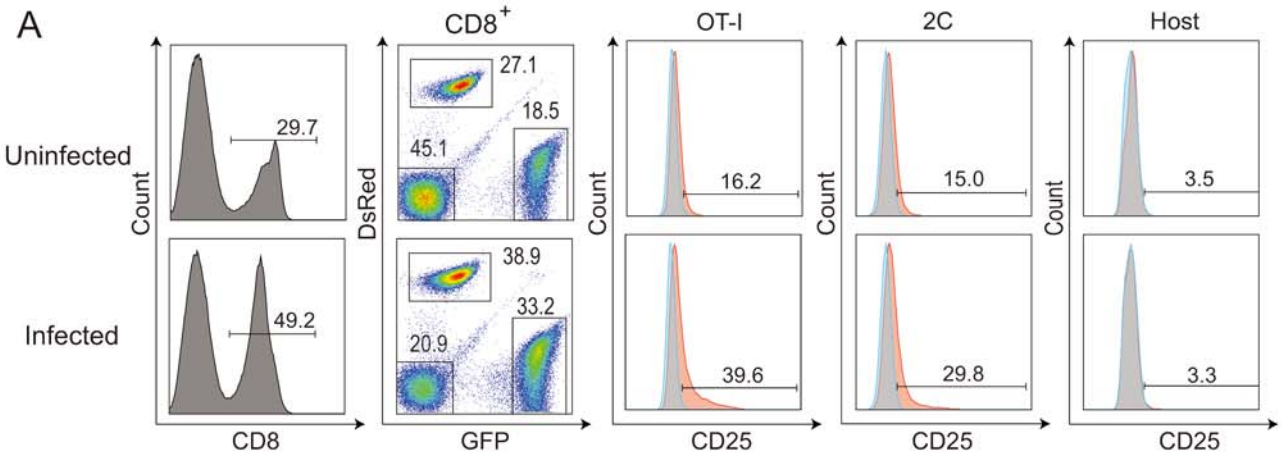
A
CD8+
OT-I
2C
Host
Uninfected
Infected
Count
DsRed
29.7
49.2
27.1
18.5
45.1
38.9
33.2
20.9
16.2
39.6
15.0
29.8
3.5
3.3
CD8
GFP
CD25

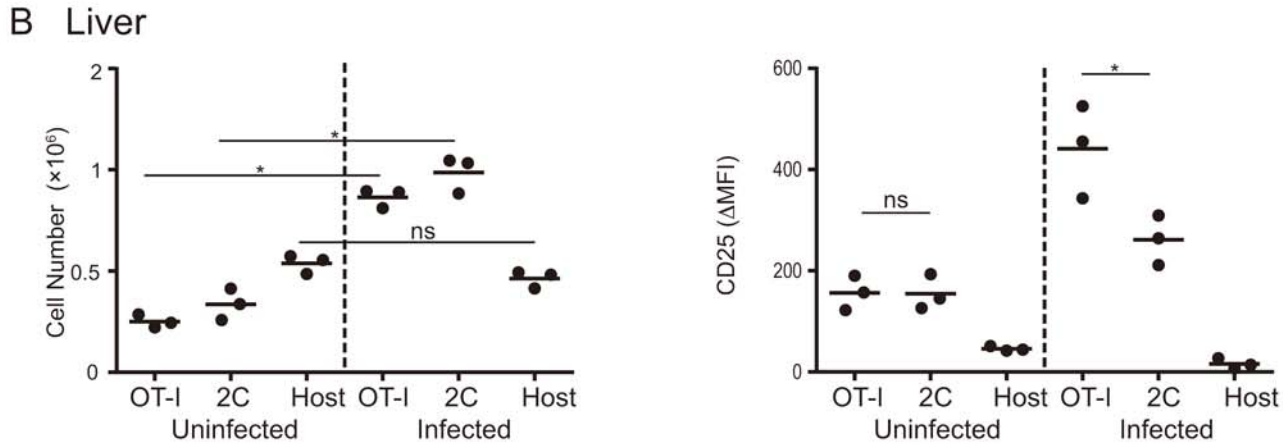
B Liver
Cell Number (×10^6)
CD25 (ΔMFI)
OT-I
2C
Host
Uninfected
Infected
ns
*

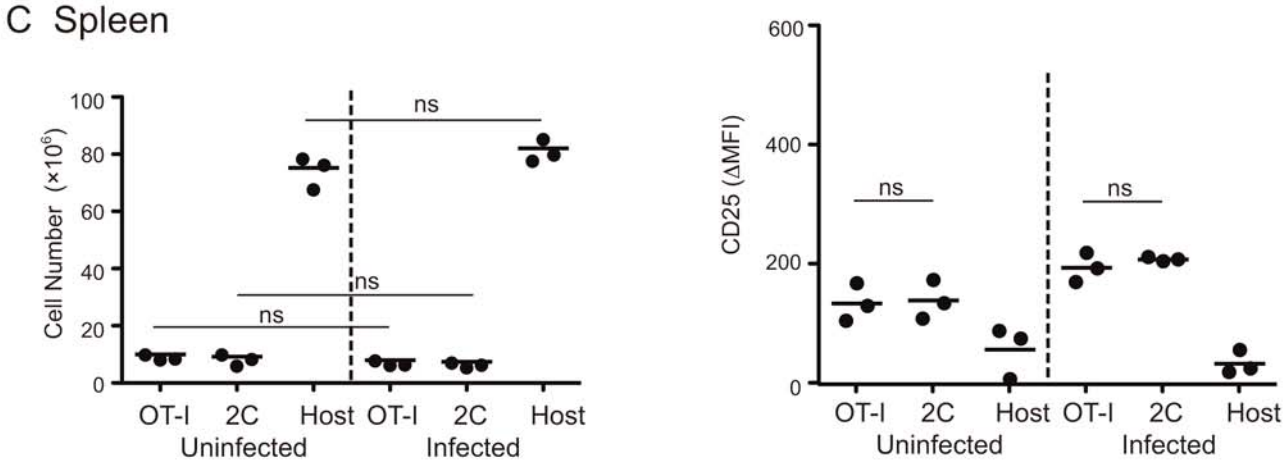
C Spleen
Cell Number (×10^6)
CD25 (ΔMFI)
OT-I
2C
Host
Uninfected
Infected
ns

Fig. 4

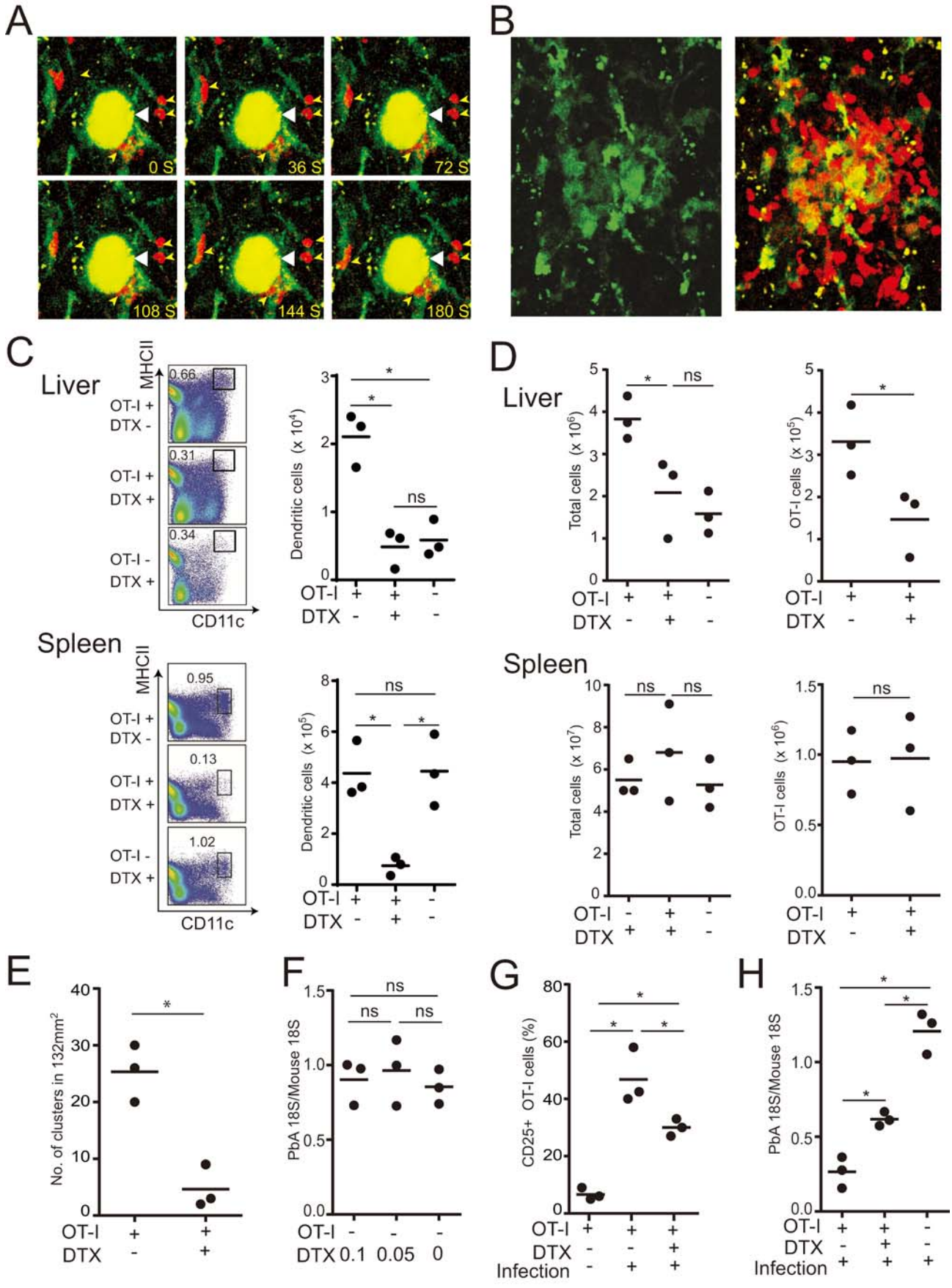
A
0 S
36 S
72 S
108 S
144 S
180 S
B
C
Liver
MHCII
CD11c
OT-I +
DTX -
OT-I +
DTX +
OT-I -
DTX +
0.66
0.31
0.34
Dendritic cells (x 10^4)
OT-I + + -
DTX - + -
Spleen
0.95
0.13
1.02
Dendritic cells (x 10^5)
D
Liver
Total cells (x 10^6)
OT-I cells (x 10^5)
Spleen
Total cells (x 10^7)
OT-I cells (x 10^6)
ns
E
No. of clusters in 132mm2
F
PbA 18S/Mouse 18S
DTX 0.1 0.05 0
G
CD25+ OT-I cells (%)
Infection
H
PbA 18S/Mouse 18S
Infection

Fig. 5